Asian Journal of Physics
Vol. 33, No 12 (2024) 825-833
Available on: www.asianjournalofphysics.com

Symmetry using Fraunhofer propagator for 2D and 3D real objects

L Mancio, R Hernandez-Delesma and A Olivares-Pérez
[1]Instituto Nacional de Astrofísica Óptica y Electrónica, calle Luis Enrique Erro No. 1,
Santa María Tonantzintla, 72840, Puebla, México

Dedicated to Prof (Dr) Daniel Malacara-Hernández

An analytical theoretical study of 2D and 3D objects using the laws of Fraunhofer diffraction is presented. The induction of symmetry following the Fourier properties of algebraic rules is demonstrated. For a completely random distribution in any type of 2D and 3D real object, there is no symmetry. However, when the real object is propagated to the far field forming the diffracted field, a particular symmetry of conjugate pairs is generated for every point as a reflection through the origin.

doi: 10.54955.AJP.33.12.2024.825-833

Keywords: Diffraction theory, Algebraic optical processing, Symmetries, Diffractive optics, Spectrum analysis.

1 Introduction

Wave propagation is well established, commonly described by the Fresnel–Kirchhoff formulation [1,2] and Fourier transformations [3,4]. Recent optical studies have applied Fourier methods in imaging and holography [5-7]. For real objects, distributions such as Gaussian, Poisson, or random exhibit symmetry only when point pairs are present, producing conjugate components across the origin. Complex (phase) objects, however, lack this symmetry. Moreover, 2D and 3D Fourier transforms can be represented in four distinct ways depending on periodicity and discreteness [8,9]. Here, we show that the far-field diffraction pattern of an asymmetric aperture reveals symmetrical behavior, providing a basis to analyze Fourier spectrum symmetries with the Fraunhofer propagator for 2D and 3D real objects.

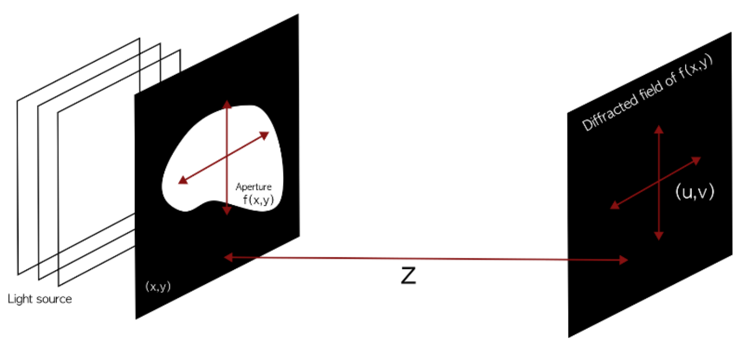

Fig 1. Diagram of Fraunhofer diffraction pattern formed by a light wave passing through an aperture.

Corresponding authors:
e mail:luis.mancio@inaoe.mx (L Mancio); rocio.hernandez@inaoep.mx (R Hernandez-Delesma);
olivares@inaoep.mx (A Olivares-Pérez).

The Eq (1) is the Fraunhofer diffraction integral, it refers to the far-field diffraction pattern observed when light waves pass through an aperture or around an obstacle, with the wavefronts considered to be parallel (Fig 1). This type of diffraction occurs when the light source and observation point are at a large distance from the diffracting object.

$$U(u, v)= \frac{e^{-jkz}}{j\lambda z}\, e^{-jk(x^2+y^2)/2z} \int_{\mathbb{R}^2} f(x, y)\, e^{-(jk(ux+vy)/z}\, dx\, dy. \quad (1)$$

Here, λ is the wavelength of the light source, $k = 2\pi/\lambda$ is the wave number, z is the observation distance. The aperture is situated in the plane (x, y) and $U(u, v)$ is the diffracted field in the plane (u, v).

Eq (1) shows that Fraunhofer diffraction is directly proportional to the Fourier transform of the aperture function Eq (2).

$$U(u, v) \propto F\,[\,f(x, y)]. \quad (2)$$

where $u = x'/\lambda z$ and $v = y'/\lambda z$.

We will now demonstrate that, regardless of the distribution of $f(x, y)$, its Fourier transform exhibits symmetries with respect to the axes, provided that $f(x, y)$ is a real function. This property is optically evident in the diffraction patterns of apertures.

2 Theory: Fourier symmetry of Fraunhofer diffraction patterns

2.1 Analytical testing of 2D case

In the 2D case, we showed that the symmetry of the conjugated pair is preserved for real 2D objects, whereas the literature considers this only in the 1D and 2D cases, with sign changes, using basic mathematical arguments [3,4,8,10]. For objects with arbitrary random distribution, their diffracted field is symmetrical [11-13]. The sampling of each vector corresponds to an independent conjugate pair. Following the logic and approach for a transformed 1D object, $F(-u, 0) = [F(u, 0)]^*$, $F(0,-v) = [\mathrm{F}(0, v)]^*$, and $F(-u,-v) = [\mathrm{F}(u, v)]^*$.

The cross-terms are more complex, since the variables u and v appear in the kernel of the Fourier transform. Following the symmetry conditions [10], we must satisfy $F(-u, v) = [F(u, -v)]^*$, or $F(u, -v) = [F(-u, v)]^*$.

The analytical proof of the conjugate-pair symmetry for 2D real objects, based on the sign change of $-u$ and $-v$, is presented below using the Fourier transform.

$$F(-u, v) = \int_{\mathbb{R}^2} f(x, y)\, e^{-2\pi j(-ux+vy)}\, dx\, dy = \int_{\mathbb{R}^2} f(x, y)\, e^{2\pi j(ux-vy)}\, dx\, dy$$

$$= \left[\int_{\mathbb{R}^2} f(x, y)\, e^{-2\pi j(ux-vy)}\, dx\, dy\right]^* = [F(u, -v)]^* \quad (3)$$

Similarly, by exchanging the sign of v we obtain the Eq (4),

$$F(u, -v) = [F(-u, v)]^* \quad (4)$$

We show that the symmetry for real objects $f(x, y)$, meets the following quadrants: $F(-u, -v) = [F(u, v)]^*$, $F(u, v) = [F(-u, -v)]^*$, $F(-u, v) = [F(u, -v)]^*$ and $F(u, -v) =[F(u, -v)]^*$. This is regardless of the distribution type and randomness of the real function.

In practice for observing the intensity from Eq (1), we calculate its complex amplitude as shown in Eq (5).

$$I(u, v) = |F(u, v)|^2 = F_r\,(u, v)^2 + F_i\,(u, v)^2 \quad (5)$$

where F_r and F_i are the real and imaginary parts, respectively in Eq (5). Let us note that F^* and F have the same intensity. Figure 1 shows the symmetries in the Fourier transform of asymmetric apertures.

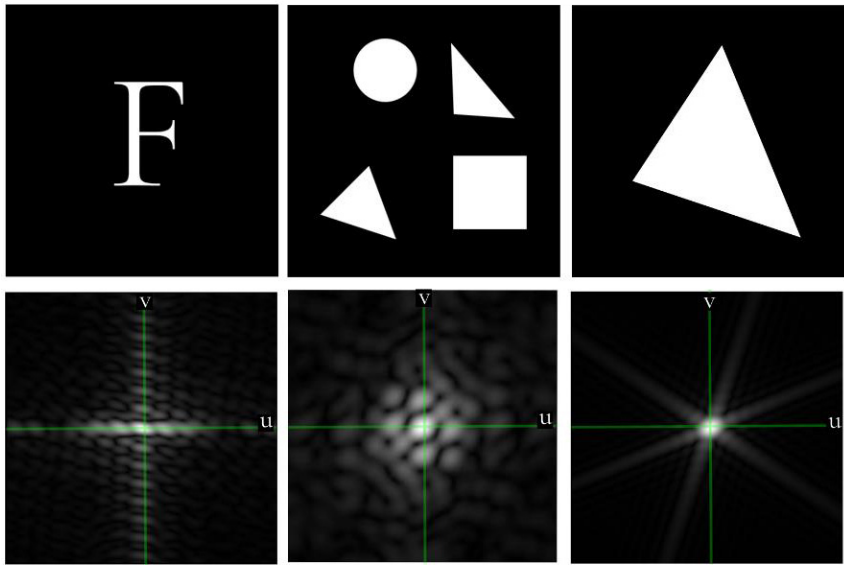

Fig 2. Asymmetric apertures and their respective Fourier transform with symmetry.

The symmetry in the diffracted field appears regardless of the shape of the aperture, whether symmetric or asymmetric, and is preserved even under conditions of randomness, representing the extreme case of asymmetry.

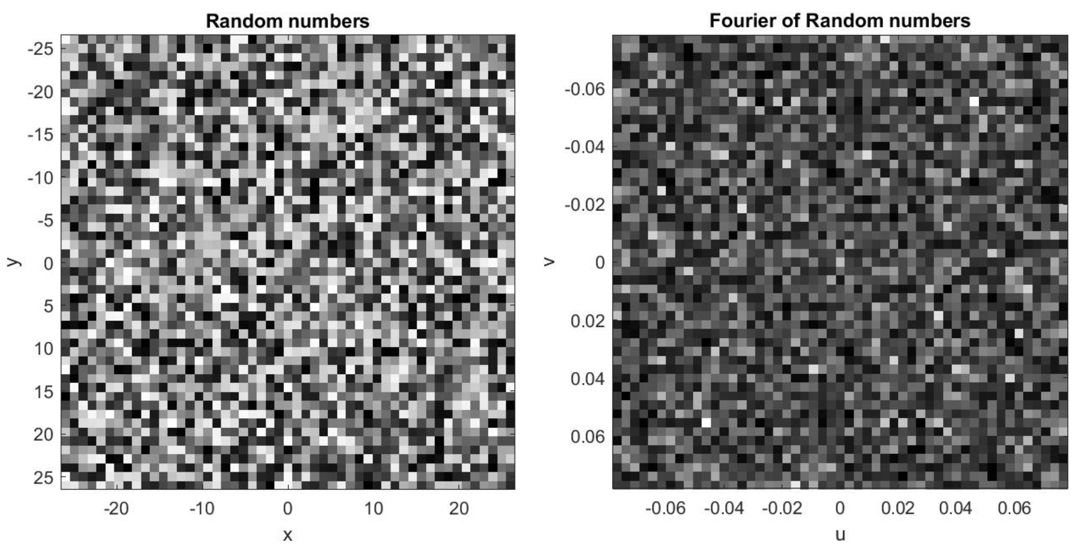

(a) (b)

Fig 3. (a) Example of a random real-valued amplitude distribution. (b) Magnitude of its Fourier transform, showing conjugate symmetry about the origin.

In Fig 4, a 180° rotation of Fig 3(b) followed by its subtraction from the original yields a zero matrix, confirming the inherent symmetry of the Fourier spectrum. Figure 5 shows the random number distribution together with its propagated spectrum, where the symmetry produced by the Fourier transform is clearly visible.

2.2 Complex objects case

In this case $g(x, y)$ is an arbitrary phase function and $f(x, y)$ represents the amplitude.

$$U(u, v) = \frac{e^{-jkz}}{j\lambda z} e^{-jk(x^2+y^2)/2z} \int_{\mathbb{R}^2} f(x, y)\, e^{-j[k(ux+vy)+g(x+y)]/z}\, dx\, dy. \tag{6}$$

The Fourier kernel is altered, and as a result, its propagation obeys the linear term plus the aggregate phase, therefore, the symmetry of the amplitude is not fulfilled.

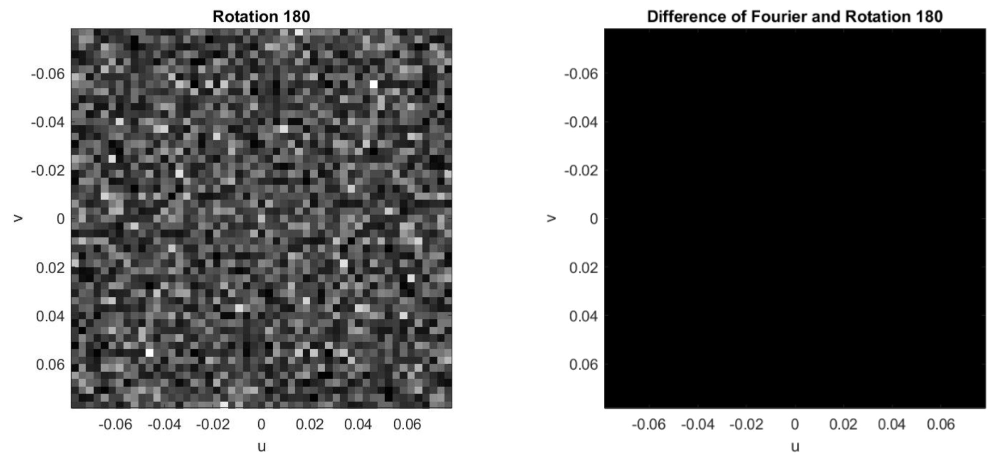

(a) (b)

Fig 4. (a) This image corresponds to Fig 3(b) rotated by 180°. (b) Result of subtracting the rotated spectrum in Fig 4(a) from the original spectrum in Fig 3(b), showing that the difference is a zero matrix and thus confirming the inherent symmetry of the Fourier spectrum.

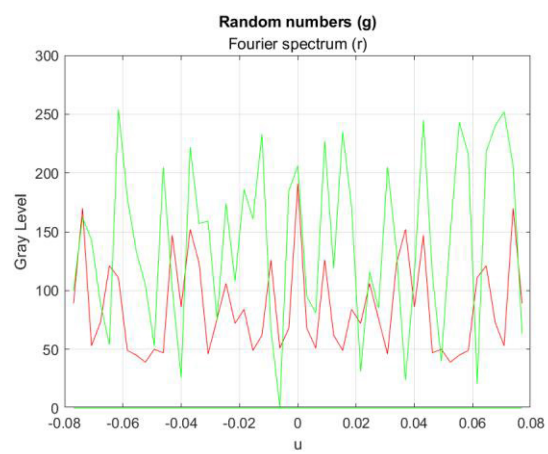

Fig 5. Cross-sectional profiles along the x-axis. The green line represents the random number distribution from Fig 3(a), and the red line represents the Fourier spectrum from Fig 3(b), showing the induced symmetry after propagation.

The image below displays a triangular shape with a phase distribution as follows:

$$g(x, y) = 10\,(x^2 + y^2) \tag{7}$$

When the object is pure phase (e.g., the triangular phase mask of Fig 6(a)), its Fourier spectrum does not exhibit conjugate symmetry, in contrast to the amplitude-only triangle of Fig 2, whose spectrum does display the expected symmetry. Similarly, Fig 7(a) shows a distribution of phase elements represented by random numbers, where each gray level corresponds to a phase value. Figure 7(b) shows Fourier transform of the phase matrix in Fig 7(a), showing no symmetry with respect to the origin.

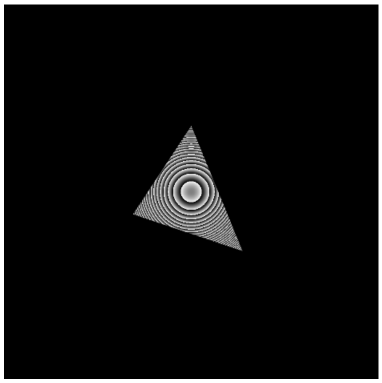

(a)

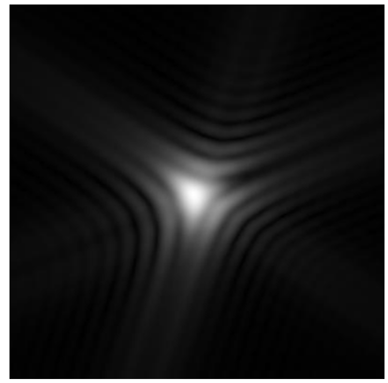

(b)

Fig 6. (a) Phase object and (b) its propagated field

2.2.1 Random phase numbers

The behavior of the distribution of random phase numbers with amplitude between 0 and 2π is shown in a general way, through propagation by applying Fourier transform.

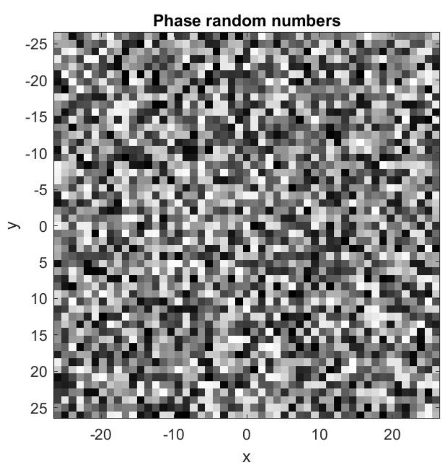

(a)

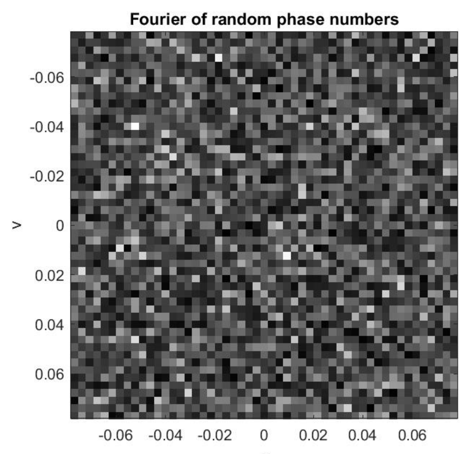

(b)

Fig 7. Distribution of (a) phase random numbers and (b) not symmetric spectrum.

Figure 8(a) shows the 180° rotation of Fig 7(b). Figure 8(b) presents the difference between the original spectrum in Fig 7(b) and its rotated version in Figure 8(a). As observed, the resulting matrix in Fig 8(b) is not a zero matrix, indicating that phase matrices do not generate symmetry with respect to the origin when propagated using the Fourier transform. In the plot shown in Fig 9, there is no symmetry observed in the propagated field of the random phase number distribution.

2.3 Analytical testing of 3D case

The 3D case follows a similar behavior. We show that the symmetry of the conjugate pair is also preserved for 3D real objects, following the same criteria for Fourier 2D objects.

All sign the combinations, i.e., $F(-u, v, w)$, $F(u, -v, -w)$, $F(u, v, w)$, $F(u, -v, w)$, $F(u, v, -w)$, $F(-u, -v, -w)$, $F(-u, v, -w)$ and $F(-u, -v, w)$ can build viable symmetries.

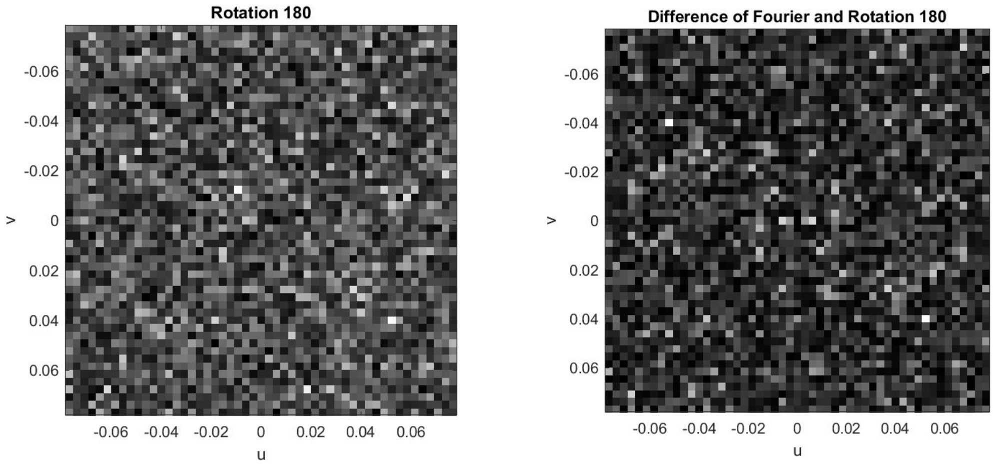

(a) (b)

Fig 8. (a) Fourier spectrum of Figure 7(b) rotated by 180° about the origin. (b) Difference between the original spectrum in Figure 7(b) and the rotated spectrum in (a). The non-zero result in (b) demonstrates that the Fourier spectrum of the phase object does not exhibit symmetry with respect to the origin.

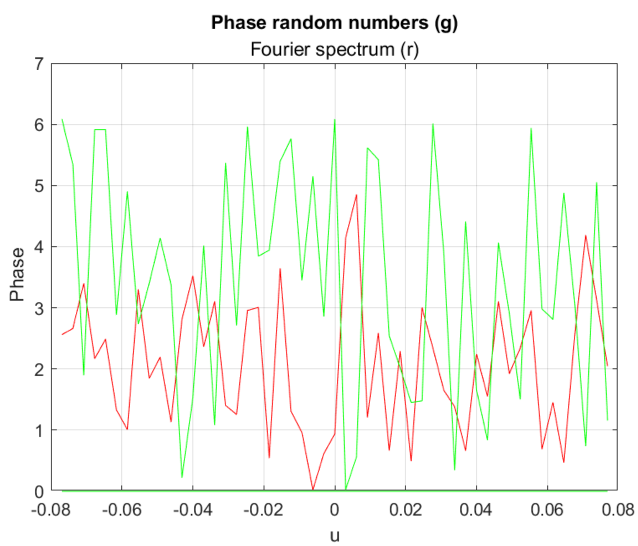

Fig 9. Cross-sectional profiles along the x-axis. The green line represents the phase random number distribution from Fig 7(a), and the red line represents the Fourier spectrum from Fig 7(b), showing no symmetry after propagation.

To preserve the symmetry, we show an octant as a particular case that must satisfy $F(-u, v, w) = F^*(u, -v, -w)$, or $F(u, -v, -w) = F^*(-u, v, w)$.

$$F(-u, v, w) = \int_{\mathbb{R}^3} f(x, y, z)\, e^{-2\pi j(-ux + vy + wz)}\, dx\, dy\, dz = \int_{\mathbb{R}^3} f(x, y, z)\, e^{2\pi j(ux - vy - wz)}\, dx\, dy\, dz$$

$$= \left[\int_{\mathbb{R}^2} f(x, y, z)\, e^{-2\pi j(ux - vy - wz)}\, dx\, dy\, dz\right]^* = [F(u, -v, -w)]^* \tag{8}$$

Equation (6) shows the symmetry of the conjugate pairs of a 3D real object. Following these steps, it can be seen, that for real objects, the following symmetries are true:

$$F(-u, v, w) = F^*(u, -v, -w) \tag{9}$$

$$F(u, -v, -w) = F^*(-u, v, w) \tag{10}$$

$$F(u, v, w) = F^*(-u,-v, -w) \tag{11}$$

$$F(u, -v, w) = F^*(-u,v, -w) \tag{12}$$

$$F(u, v, -w) = F^*(-u,-v, w) \tag{13}$$

$$F(-u, -v, -w) = F^*(u, v, w) \tag{14}$$

$$F(-u, v,-w) = F^*(u, -v, w) \tag{15}$$

$$F(-u,-v, w) = F^*(u, v, -w) \tag{16}$$

The visualization of the symmetry in the propagated field of a 3D object is presented in Fig 10, which represents Eqs (9-16). We generated a 3D real amplitude object in Matlab R2022a using the function, $f = f_1 \cdot f_2 + f_3$, where $f_1 = \exp\left(\sin(k(x + z^2)\right)$, $f_2 = \exp\left(k(x + 3y - z)\right)$ and $f_3 = \exp\left(\cos(kz^2)\right)$ with $k = 2\pi/3$.

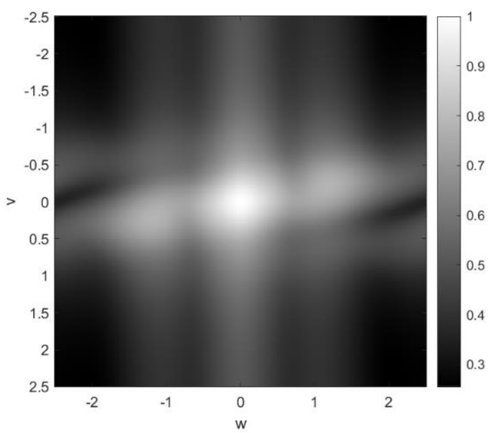

(a)

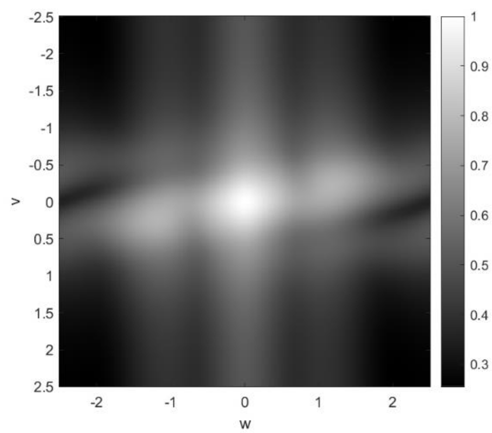

(b)

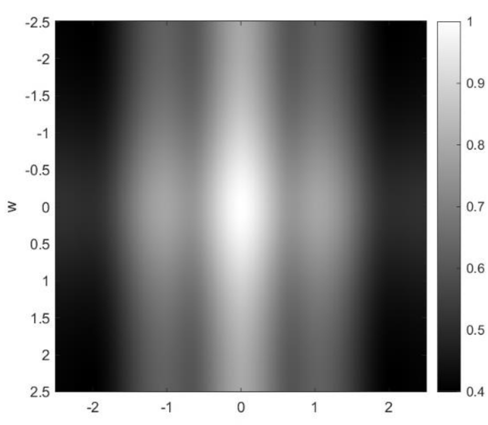

(c)

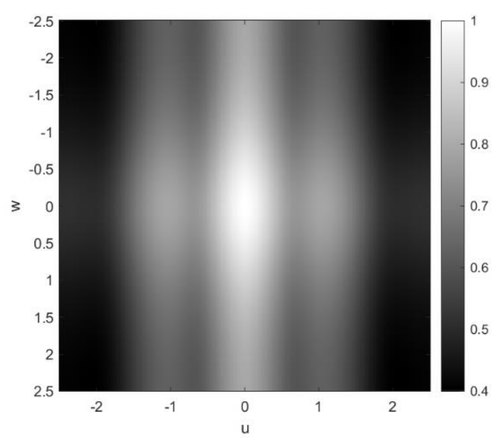

(d)

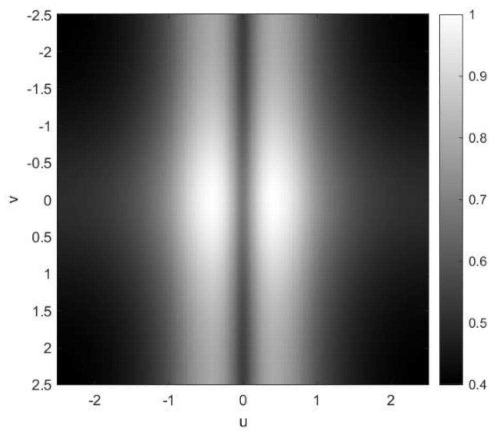

(e)

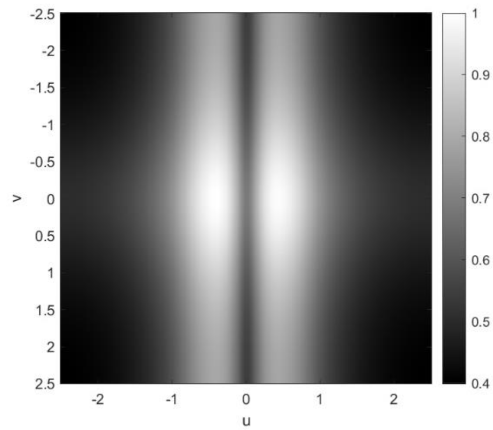

(f)

Fig 10. Projections of the Fourier transform of the amplitude object: (a) section in the x-plane at $u = -2.45$ and (b) its reflection at $u = 2.45$; (c) section in the y-plane at $v = -2.45$ and (d) its reflection at $v = 2.45$; (e) section in the z-plane at $w = -2.45$ and (f) its reflection at $w = 2.45$. These projections numerically demonstrate the symmetry of the propagated field of the amplitude object.

After computing the 3D Fourier transform, we extracted planar slices at fixed u, v and w from negative to positive values to verify the predicted conjugate symmetry across each axis. The functions f_1, f_2, and f_3 were chosen to enhance the visualization of the propagation behavior and to verify the symmetry in the Fourier field at the limits of u, v, and w. A mask with more sampling points was applied to enhance the visualization of the Fourier field.

3 Discussion

This work explored the connections between the Fourier transform and diffractive optics. The symmetry inherent in the Fourier transform is made evident through direct calculations, using the property of reflection in Fourier space for 2D and 3D cases, of amplitude objects. The Fourier kernel has a linear character that causes amplitude objects to acquire symmetry as observed in section 2.1 when propagating. However, for phase objects this linearity is lost due to the additional phase term included in the kernel, as shown in Eq(6), section 2.2. In other words, once the kernel is modified by the phase element, its propagation no longer preserves the symmetry that is characteristic of amplitude objects.

This Hermitian (conjugate) symmetry is particularly valuable for reducing computational complexity, minimizing both processing time and memory usage when storing complex data. The associated Fourier-based methods that exploit this property—such as storing only half of the non-redundant spectrum or reconstructing coefficients by mirroring—are especially useful in handling large data sets or computationally intensive tasks, making Fourier-based approaches essential for efficient and accurate analysis in diffractive optics. Moreover, the interaction between the mathematical framework of Fourier analysis and the physical behavior of light diffraction underscores the broad usefulness of Fourier techniques in both theoretical and practical applications within the realm of diffractive optics.

3 Conclusions

For real objects propagated under Fraunhofer conditions, the transformed fields inherit conjugate-symmetry vectors about lines through the origin, independently of the distribution type, randomness, or dimensionality (2D/3D). This physical property of conjugate symmetry is conserved in 1D, 2D, and 3D space.

In the 2D and 3D domain it is evident in the field of holography, which can store complex information to retrieve information giving the possibility of recovering the initial information of the object. On the other hand, in the field of computational data (complex numbers), it is possible to retrieve information because the transformation has an exact inverse.

For phase objects, the proposed symmetries are not fulfilled due to the linear alteration of the Fourier kernel. But this asymmetry still allows for an inverse transform, the accuracy of this transform depends on kernel degradation. When the object is propagated, its diffracted pattern is usually expressed with amplitude and phase, and we only see the magnitude of the result. More studies are needed to explore symmetries in the phase map.

Acknowledgements

For The research described in this publication was made possible in part by INAOE, Instituto Nacional de Astrofisica Optica y Electronica, for the equipment and laboratory facilities, as well as for the support with providing supplies. We would also like to extend our gratitude to CONAHCYT, Consejo Nacional de Humanidades Ciencias y Tecnologias, for the financial support given to the students involved in this project.

References

1. Born M, Wolf E, Principles of optics: electromagnetic theory of propagation, interference and diffraction of light, (Cambridge University Press., New York), 1999.
2. Klein M V, Furtak T E, Optic, (John Wiley & Sons, New York), 1986.
3. Bienenstock A, Ewald P P, Symmetry of Fourier Space, *Acta Cryst*, 15(1962)1253–1261.
4. Rahman M, Applications of Fourier Transforms to Generalized Functions, (WIT Press., Boston), 2011.
5. Sun R, Ding Y, Kuang J, Cheng J, Buczynski R, Liu W, Non-phase-shift Fourier single-pixel imaging with conjugate symmetry of the Fourier spectrum and ADMM-based image inpainting, *Opt Lett*, 50(2025)6169–6172.
6. Mustafi S, Latychevskaia T, Fourier Transform Holography: A Lensless Imaging Technique, Its Principles and Applications, *Photonics*, 10(2023)153; /doi.org/10.3390/photonics10020153.
7. Fienup J R, Fourier-optics imaging analysis with ABCD matrices: tutorial, *J Opt Soc Am A*, 41(2024)2361–2370.
8. Two-Dimensional Fourier Transform – Harvey, http://fourier.eng.hmc.edu/e101/lectures/Image_Processing/node6.html.
9. Urzúa A R, Ramos-Prieto I, Moya-Cessa H M, Integrated optical wave analyzer using the discrete fractional Fourier transform, *J Opt Soc Am B*, 41(2024)2358–2365.
10. The University of Edinburgh, School of Physics and Astronomy, Symmetry of Fourier Transform, http://www2.ph.ed.ac.uk/~wjh/teaching/Fourier/documents/symmetry.pdf.
11. Lehmer D H, Random number generation on the BRL high-speed computing machines, *Math Rev*, 15(1954)559.
12. Van-Gelder A, Some new results in pseudo-random number generation, *J ACM*, 14 (1967)785–792.
13. Payne W H, Rabung J R, Bogyo T P, Coding the Lehmer pseudo-random number generator, *Commun ACM*, 12(1969)85–86.

[*Received*: 30.11.2024; *rev recd*: 29.12.2024; *accepted*: 30.12.2024]

Luis Mancio

Physicist–Mathematician graduated from the National Polytechnic Institute (IPN) with a Master's degree in Optics from the National Institute of Astrophysics, Optics and Electronics (INAOE), Mexico. Specialized in computational holography applied to optical measurement and wavefront reconstruction. Contributor to three peer-reviewed publications.

Angélica Rocío Hernández Delesma

Physicist graduated from the Universidad Autónoma de Chiapas with a Master's degree in Optics from the National Institute of Astrophysics, Optics and Electronics (INAOE), Mexico. Currently a Ph D candidate in Optics at INAOE and a member of the Holography Research Group, focusing on digital and analog holography for optical measurement and wavefront analysis. Contributor to two peer-reviewed publications.

Arturo Olivares-Pérez

Ph D graduate from the Center for Optical Research (CIO) in 1993. Dr Olivares-Pérez is a researcher at the National Institute of Astrophysics, Optics, and Electronics (INAOE), in the Department of Optics, specializing in holography and photosensitive materials. Dr Olivares-Pérez is Advisor to 12 doctoral students, 14 master's students, and 13 undergraduate students, with over 180 publications.